

Enhanced Responsivity and Detectivity Values of Short 30-period InAs/GaSb Type-II Infrared Photodetectors with Reduced Device Areas

Hsuan-An Chen^{1,2}, Tung-Chuan Shih¹, Hsuan-You Chen³ and Shih-Yen Lin^{1,2,3*}

¹ Academia Sinica

Research Center for Applied Sciences

128, Sec. 2, Academia Rd., Taipei City 11529, Taiwan

Phone: +886-2-2787-3187 *E-mail: shihyen@gate.sinica.edu.tw

² National Taiwan Univ.

Graduate Institute of Electronics Engineering

No.1, Sec. 4, Roosevelt Rd., Taipei City 10617, Taiwan

³ National Taiwan Ocean Univ.

Institute of Optoelectronic Sciences

No. 2 Pei-Ning Road, Keelung 20224, Taiwan

Abstract

Enhanced responsivity and detectivity values are observed for a short 30-period InAs/GaSb type-II superlattice infrared photodetector with reduced device areas. With cut-off wavelength at 4 μm , the device with the smallest device area exhibits the 10 K responsivity value of 15 mA/W and the corresponding detectivity value of $1.7 \times 10^{12} \text{ cm} \cdot \text{Hz}^{1/2} / \text{W}$ at 3.6 μm . The thermal images obtained by using a single-detector raster scan system have demonstrated the potential of the device for this application.

1. Introduction

The requirements for the next-generation infrared photodetector would be (a) high operation temperatures, (b) insensitivity to incident light polarizations, (c) uniform wafer uniformity and (d) tunable detection wavelengths. Among all the candidates, the most promising device would be InAs/GaSb type-II superlattice infrared photodetectors (T2SL). The first T2SL infrared photodetector was demonstrated by Mailhot and Smith at the year 1987 [1]. By controlling the individual layer thickness and composition of the superlattice structures, different detection wavelengths can be obtained by using the T2SL structures [2]. With the photo-voltaic operation mode of the InAs/GaSb T2SL infrared photodetector, high operation temperature is expected for the device [3].

However, compared the matured growth technique of GaAs/(AlGa)As hetero-structures for QWIPs, the major challenges for the development of InAs/GaSb T2SLs lies on (a) As/Sb interface treatment for wafer preparation and (b) dark current depression for the small-bandgap devices. On the other hand, hundreds of superlattice periods are usually required for the T2SL infrared photodetectors due to its low quantum efficiency, which would further increase the difficulty for epitaxy growth. In this report, we have demonstrated improved responsivity and detectivity values of short 30-period InAs/GaSb T2SL infrared photodetectors with reduced device area. The thermal images obtained by

using the single-detector raster scanning system are also demonstrated.

2. Results and Discussions

All Samples presented in this report are grown by using RIBER C21 solid-state Molecular Beam Epitaxy system (MBE) on 2 inch *n*-type (100) GaSb substrates ($n = 5 \sim 10 \times 10^{17} \text{ cm}^{-3}$, Te-doped). The structures are shown in Table I., the SLs photodiode structure consists of the active region 30-periods InAs (5 MLs) / GaSb (5 MLs) SLs with InSb (1 MLs) strain compensator inserted between GaSb-to-InAs interfaces embedded in the undoped 700 nm GaSb layer. 200 nm *p*-type GaSb ($p = 3 \times 10^{19} \text{ cm}^{-3}$, Be-doped) is grown on top of the SL structure as the contact layer. The growth temperature for the SL structure is 400 °C and the V/III ratios for InAs and GaSb are 10 and 5, respectively. After growth, the device fabrication was performed by using standard photolithography techniques. The mesa formation was achieved by using $\text{CH}_3\text{COOH} / \text{HNO}_3 / \text{HF}$ etching solution. Devices with different mesa sizes 300 \times 300, 200 \times 200 and 100 \times 100 μm^2 are fabricated for comparison. After mesa formation, the samples were passivated by soaking in the $(\text{NH}_4)_2\text{S}$ aqueous solution. To protect the passivated surfaces, the photo-resist SU-8 was spin coated on the sample and then hard baked at 200 °C with 30 minutes as the passivation protection layer. After Ti (20 nm) / Au (200 nm) metal deposition, the sample is annealed at 350 °C for Ohmic contact formation. The window openings for light detection of the devices with 300 \times 300, 200 \times 200 and 100 \times 100 μm^2 mesas are 200 \times 200, 120 \times 120 and 40 \times 40 μm^2 , which are referred as Devices A, B and C, respectively.

Table I. The Wafer Structure of the T2SL sample.

p-GaSb 200 nm ($p = 3 \times 10^{19} \text{ cm}^{-3}$, Be-doped)
<i>i</i> -GaSb 350 nm
30 \times (1MLs InSb / 5MLs InAs / 5MLs GaSb)
<i>i</i> -GaSb 350 nm
<i>n</i>-GaSb Sub 500 μm ($n = 5 \sim 10 \times 10^{17} \text{ cm}^{-3}$, Te-doped)

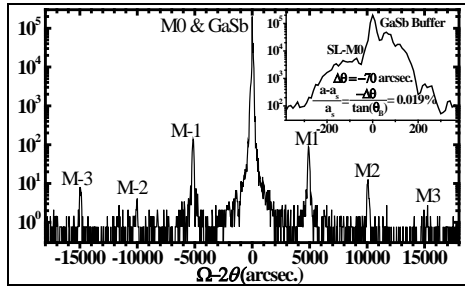


Fig. 1 The X-ray diffraction curve of the T2SL sample. The enlarged curve near the substrate peak is shown as an inset figure.

The X-ray diffraction curve of the sample measured by using the double crystal X-ray diffraction system is shown in Fig. 1. Since InAs is -0.62 % mismatched to GaSb, the additional tensile stress may result in increasing defect formation in the SL structure. Therefore, with additional 1 ML InSb strain compensator layers inserted between each InAs-on-GaSb interface, the $m = 0$ satellite peak would almost coincide with the GaSb substrate peak. The enlarged curve shown as an inset reveals that only minor compressive strain with 0.019 % lattice mismatch is obtained for the sample. The InSb layers also act as an effective scarring layer for the commonly observed As-for-Sb exchange at the As/Sb interfaces. The abrupt As/Sb interfaces would lead to clear satellite peaks observed in the figure.

The 10 K spectral responses of the three devices measured at $V = 0$ V are shown in Fig. 2 (a). As shown in the figure, the responsivity values at $3.6 \mu\text{m}$ would increase from 0.12, 0.5 to 15 mA/W for Devices A, B and C, respectively. Since no external biases are applied to the devices, the photo-excited electron-hole pairs are separated by the build-in electric field of the P-N junction. Holes should transport directly to the metal contact rims instead of vertically flowing to the p-GaSb layer and then collected by the metal electrode. The increasing device areas would also increase the carrier transporting length in the SL structure such that higher carrier recombination rate is observed for the device with larger device areas. The results suggest that besides increasing the SL period number, the other approach to increase the responsivity values of the T2SL infrared photodetector is to shrink its device areas. With the increasing responsivity values with decreasing device areas, the 10 K detectivity values at $3.6 \mu\text{m}$ of Devices A, B and C would increase from 2.4×10^{10} , 3.6×10^{11} to 1.7×10^{12} $\text{cm} \cdot \text{Hz}^{1/2} / \text{W}$, respectively.

The main application of the device is in thermal imag-

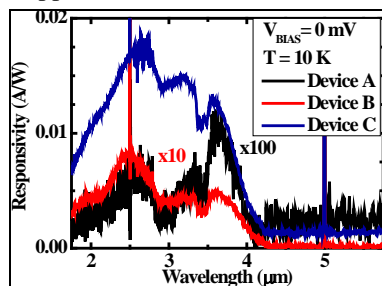


Fig. 2 The 10 K spectral responses of Devices A, B and C measured at $V = 0$ V.

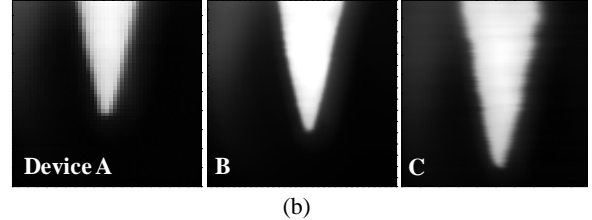
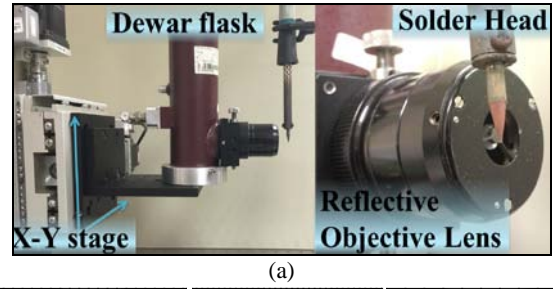


Fig. 3 (a) The single-detector raster scanning system and (b) the thermal images of a hot solder head tip obtained by using Devices A, B and C.

ing. We have established a single-detector raster scanning system to demonstrate this possibility. The system set is shown in Fig. 3 (a). By using an L-N₂ cooled Dewar flask mounted with a reflective objective lens, the three devices are cooled down to 77 K for thermal image scanning by using a computer-controlled X-Y stage. Since the reflective objective lens is mounted to the Dewar flask, the magnification of the thermal image is 1 \times and the resolution of the thermal images is limited by the window sizes of the devices. The thermal images of the hot solder head tip with different resolutions 200×200 , 120×120 and $40 \times 40 \mu\text{m}^2$ for Devices A, B and C, respectively, are shown in Fig. 3 (b). The results suggest that besides improved responsivity and detectivity values, better thermal resolution can be obtained with reduced device areas.

3. Conclusions

We have demonstrated enhanced responsivity and detectivity values for 30-period InAs/GaSb T2SL infrared photodetectors with reduced device areas. With longer transporting lengths, high carrier recombination probability would take place in the SL structure. The demonstration of thermal images obtained by using a single-detector raster scanning system has revealed the potential of the T2SL infrared photodetector for this application.

Acknowledgements

This work was supported in part by MOST project NSC 102-2221-E-001-032-MY3, and the CSIST project XV04G02P-CS.

References

- [1] D. L. Smith and C. Mailhot, J. Appl. Phys., **62**, (1987)pp. 2545.
- [2] M. Razeghi, Y. Wei, A. Gin, G. J. Brown, and D. Johnstone, in Proc. SPIE, San Jose, CA, **4650**, (2002) pp. 111-116.
- [3] E. R. Youngblade, J. R. Meyer, C. A. Hoffman, F. J. Bartoli, C. H. Grein, P. M. Young, H. Ehrenreich, R. H. Miles, and D. H. Chow, Appl. Phys. Lett., **64**, (1994) pp. 3160-3162.